Effect of low nitrogen concentrations on the electronic properties of $InAs_{1-x}N_x$

A. Patanè,[1,*] W. H. M. Feu,[1] O. Makarovsky,[1] O. Drachenko,[2] L. Eaves,[1] A. Krier,[3] Q. D. Zhuang,[3] M. Helm,[2] M. Goiran,[4] and G. Hill[5]

[1]*School of Physics and Astronomy, The University of Nottingham, Nottingham NG7 2RD, United Kingdom*

[2]*Institute of Ion Beam Physics and Materials Research, Forschungszentrum Dresden-Rossendorf, 01314 Dresden, Germany*

[3]*Physics Department, Lancaster University, Lancaster LA1 4YB, United Kingdom*

[4]*Laboratoire National des Champs Magnétiques Intenses, 143 Av. de Rangueil, 31432 Toulouse, France*

[5]*Department of Electronic and Electrical Engineering, University of Sheffield, Sheffield S3 3JD, United Kingdom*

(Received 5 June 2009; revised manuscript received 27 July 2009; published 16 September 2009)

We report cyclotron resonance (CR), transverse magnetoresistance (MR), and Hall effect studies of a series of *n*-type $InAs_{1-x}N_x$ epilayers grown on GaAs with x up to 1%. The well-resolved CR absorption lines, the classical linear MR, Shubnikov–de Haas magneto-oscillations, and negative MR revealed in our experiments provide a means of probing the effect of the N atoms on the electronic properties of this alloy system and reveal qualitative differences compared to the case of the wider gap III-N-V compounds, such as $GaAs_{1-x}N_x$. In $GaAs_{1-x}N_x$ electron localization by N levels that are resonant with the extended band states of the host crystal act to degrade the electrical conductivity at small x ($\sim$0.1%). These phenomena are significantly weaker in $InAs_{1-x}N_x$ due to the smaller energy gap and higher energy of the N levels relative to the conduction band minimum. In $InAs_{1-x}N_x$ the electrical conductivity retains the characteristic features of transport through extended states, with electron coherence lengths ($l_\varphi \sim 100$ nm at 2 K) and electron mobilities ($\mu = 6 \times 10^3$ cm^2 V^{-1} s^{-1} at 300 K) that remain relatively large even at $x = 1\%$.

DOI: 10.1103/PhysRevB.80.115207 PACS number(s): 75.47.−m, 72.20.−i, 72.80.Ey, 76.40.+b

I. INTRODUCTION

The strong modification of the conduction band structure of III-V semiconductors by a low-concentration (<10%) of N atoms[1] is a problem of fundamental interest in solid state physics[2–5] and has opened up interesting prospects for innovative technologies in electronics and optoelectronics.[6–10] In dilute nitride III-N-V alloys, the resonant interaction between the strongly localized N-levels and the extended conduction band states of the III-V host crystal provides a means of tailoring important material parameters, such as the energy gap, E_g. Interest has focused more recently on narrow energy-gap semiconductors, such as InAs, which has a band gap $E_g = 0.35$ eV at room temperature ($T = 300$ K). The incorporation of nitrogen in this compound induces large relative changes of E_g,[10–17] thus, making the $InAs_{1-x}N_x$ alloy an attractive alternative to more established materials, such as $Hg_{1-y}Cd_yTe$, for infrared (IR) gas sensing and security applications.

$InAs_{1-x}N_x$ has proved to be a useful material for fabricating alloys with a photon absorption energy in the IR that can be tuned by the N concentration. However, despite many studies of the optical properties of $InAs_{1-x}N_x$, less attention has been paid to the effect of nitrogen incorporation on the electrical conductivity.[16–19] This is partly due to the need for structures in which the $InAs_{1-x}N_x$ alloy is grown on semi-insulating substrates, such as GaAs, and partly due to the problem of measuring the electrical properties of narrow-band gap semiconductor epilayers, namely the presence of two distinct parallel conduction channels, one due to a surface accumulation layer and the other to the bulk layer.[20,21] It is not obvious *a priori* that conventional models of electron transport can be applied to highly mismatched III-N-V alloys in which the electronegative N atoms act to localize the conduction electrons and thus reduce the Γ-conduction band character of the states at the Fermi level. Furthermore, important aspects of the electronic properties of $InAs_{1-x}N_x$, such as the electron effective mass and the effect of compositional disorder on electron scattering rates, are still largely unexplored. A better knowledge of these properties is essential for testing existing models of the electronic properties of III-N-V alloys[2–5,22,23] and for exploiting $InAs_{1-x}N_x$ in functional devices.

In this paper, we report cyclotron resonance (CR), transverse magnetoresistance (MR) and Hall effect studies of a series of $InAs_{1-x}N_x$ epilayers grown on semi-insulating GaAs with x up to 1%. Our data and analysis indicate that the effect of the nitrogen on the electronic properties of the narrow-band gap $InAs_{1-x}N_x$ alloy is qualitatively different from that observed in wider gap III-N-V compounds, such as $GaAs_{1-x}N_x$, where scattering and localization of electrons by crystal defects and/or N levels resonant with the extended band states tend to fragment the conduction band[2–5] and degrade the electrical conductivity at relatively low N-concentrations ($x \sim 0.1\%$).[6,19,22,23] In the $InAs_{1-x}N_x$ alloy, N-atoms and N-N pairs are located at higher energies in the conduction band ($\sim$1 eV) than in $GaAs_{1-x}N_x$ ($\sim$0.1 eV).[5] Hence, the strength of resonant electron scattering is significantly weaker. We investigate (i) the contribution to the electronic conduction of the bulk $InAs_{1-x}N_x$ epilayer and the two-dimensional surface accumulation layer; (ii) a classical linear MR effect due to inhomogeneities in $InAs_{1-x}N_x$ over characteristic length scales much larger than the carrier mean free path; (iii) scattering times sufficiently long to reveal Shubnikov–de Haas (SdH) magneto-oscillations due to the surface accumulation layer, and (iv) sharp CR absorption lines arising from electrons in the bulk $InAs_{1-x}N_x$ over the N concentration range $0 \leq x \leq 1\%$.

II. SAMPLES AND EXPERIMENTS

Our series of $InAs_{1-x}N_x$ epilayers were all grown by molecular beam epitaxy on semi-insulating (100)-oriented GaAs substrates. They have thicknesses t of ~ 1 μm and $x=0\%$, 0.2%, 0.4%, 0.6%, and 1%. The surface reconstruction was monitored by *in situ* reflection high energy electron diffraction (RHEED), while the substrate temperature was measured using an infrared pyrometer calibrated with the surface reconstruction transitions at a fixed As flux. A Veeco UNI-Bulb rf plasma source was used as nitrogen source. It was set at a radio frequency power of 160 W with a nitrogen flux of 5×10^{-6} mbar for all epilayers. This setting was precisely precalibrated to give efficient dissociation of N_2 into atomic nitrogen and to keep a low density of ionized molecular species, which are known to degrade the crystal quality.[24] The N content ($x=1\%$, 0.6%, 0.4%, 0.2%, and 0%) in each epilayer was controlled by setting the growth temperature, T_G, and the growth rate, r_G, to given values in the ranges $T_G=400-460$ °C and $r_G=0.3-1$ μm/h, and by keeping a minimum As flux. Our control sample, i.e., an InAs epilayer, was grown at $T_G=460$ °C. The Hall mobility for this sample is $\mu_H=4\times10^4$ cm^2 V^{-1} s^{-1} at $T=77$ K, which is comparable to that reported for InAs grown on GaAs under optimum growth conditions, i.e., μ_H varies between 1×10^4 and 8×10^4 cm^2 V^{-1} s^{-1} at 77 K for film thicknesses in the range 0.05 to 5 μm and $T_G=490$ °C.[21] For $x>0\%$, the growth conditions were chosen to ensure an accurate control of the N-content and to retain good optical quality of the epilayers. In previous studies,[12] we observed that nitrogen is not incorporated in InAs for $T_G\geq460$ °C, and that the optical properties of $InAs_{1-x}N_x$ tend to degrade for $T_G\leq380$ °C. Similar behavior was observed previously in the dilute nitride (GaIn)(NAsSb) and attributed to the increased formation of point defects, such as arsenic antisites, at low growth temperatures.[25]

To measure the N content, x, we performed high resolution x-ray diffraction measurements using a Bede QC200 diffractometer. This confirmed a relaxation of the crystal lattice by ~98% in all $InAs_{1-x}N_x$ epilayers. For photoluminescence (PL) experiments, the as-grown samples were excited by the 514.5 nm line of an Ar^+ laser at power densities $P<20$ W cm^{-2}. The luminescence was collected using CaF_2 lenses and dispersed by a 0.3 m Bentham M300 monochromator. The radiation was then detected using a cooled ($T=77$ K) InSb photodiode detector and a Stanford Research (SR850) digital lock-in amplifier. These measurements showed that the low temperature ($T=4.2$ K) PL emission red shifts from 0.42 eV to about 0.35 eV with increasing x from 0 to 1%, in qualitative agreement with optical data reported previously for $InAs_{1-x}N_x$ epilayers grown on other substrates (e.g., InP and InAs) or using different growth techniques.[11–13,15] A strong and broad PL emission centered at around 0.3 eV was also measured at room temperature ($T=300$ K) in the $InAs_{1-x}N_x$ sample with $x=1\%$. For further details on the PL properties of all samples, see Ref. 26.

The CR magnetotransmission spectra of the as-grown samples were measured using a pulsed magnet field B up to 55 T with a total pulse length of 100 ms. The signal was measured at fixed wavelengths, $\lambda=103$ μm and $\lambda=75$ μm, using semiconductor quantum cascade lasers (QCLs) (Refs. 27 and 28) as terahertz sources and a Ga-doped Ge photoconductor as detector. For details of the QCLs used in our experiment, see Ref. 27. The CR experiments were performed in the Faraday configuration, i.e., with the laser beam parallel to the direction of B and to the growth axis, z. The MR studies up to static fields of 14 T were carried out on Hall bars of length, L, and width, w, of 1250 and 250 μm, respectively. To fabricate the Hall bars, the samples were spun with photoresist and patterned with a Hall bar mesa mask by standard photolithography. The mesas were etched for 2.5 min using a sulphuric peroxide etch ($H_2SO_4:H_2O_2:H_2O$, 1:8:80), giving a mesa etch depth of 1.2 μm. After the mesa resist had been removed using solvents, the resist was again spun onto the sample and patterned using an ohmic contact mask. The exposed contact regions were cleaned using a deoxidizing etch of 19:1 $H_2O:NH_4OH$, then placed in an evaporator at 1.5×10^{-6} mbar. Metal contacts consisting of 10 nm of titanium followed by 200 nm of gold were deposited onto the samples to provide Ti-Au ohmic contacts.

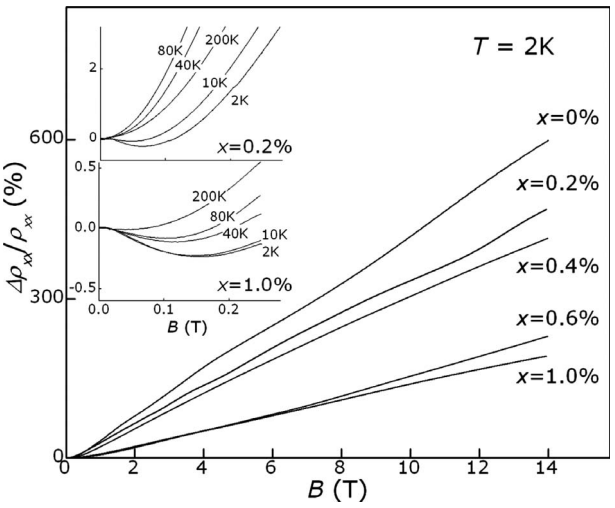

FIG. 1. Transverse MR, $\Delta\rho_{xx}/\rho_{xx}$, as a function of B for all samples ($T=2$ K). Inset: negative MR and its T dependence for $x=0.2\%$ and 1%.

III. TRANSVERSE MAGNETORESISTANCE

Figure 1 shows the low temperature ($T=2$ K) transverse MR, defined as $\Delta\rho_{xx}/\rho_{xx}=[\rho_{xx}(B)-\rho_{xx}(0)]/\rho_{xx}(0)$, as a function of B applied parallel to the growth axis, z. All of our $InAs_{1-x}N_x$ samples reveal a positive linear MR at high B (>1 T) and a weak negative MR at $B\sim0.1$ T (inset of Fig. 1). Samples with $x<0.4\%$ also show a weak oscillatory modulation of ρ_{xx}. The negative MR and the oscillatory component of ρ_{xx} quench with increasing temperature, whereas the linear positive MR effect is only weakly affected by temperature. Figure 2 shows the B dependence of $\Delta\rho_{xx}/\rho_{xx}$ at different T for two representative $InAs_{1-x}N_x$ epilayers with $x=0.2\%$ and 1%. To reveal the oscillatory component of $\rho_{xx}(B)$ and its T dependence, in the bottom inset of Fig. 2 we plot the dependence of $\Delta\rho_{xx}/\rho_{xx}$ on B after subtracting a

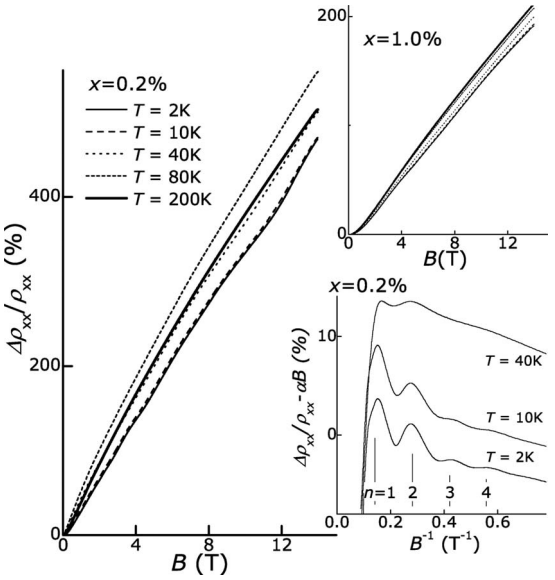

FIG. 2. Transverse MR, $\Delta\rho_{xx}/\rho_{xx}$, as a function of B for $InAs_{1-x}N_x$ samples with $x=0.2\%$ and $x=1\%$ ($T=2$, 10, 40, 80, and 200 K). Bottom inset: dependence of $\Delta\rho_{xx}/\rho_{xx}$ on $1/B$ after subtraction of a background linear in B, i.e., $\Delta\rho_{xx}/\rho_{xx}-\alpha B$, where α is a constant. Maxima in $\Delta\rho_{xx}/\rho_{xx}$ are indicated by the integer n.

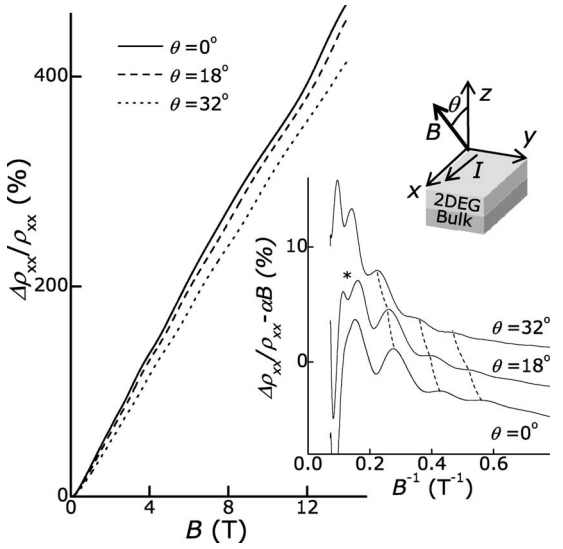

FIG. 3. Transverse MR, $\Delta\rho_{xx}/\rho_{xx}$, as a function of B tilted at angle θ relative to the growth axis z for an $InAs_{1-x}N_x$ sample with $x=0.2\%$ ($T=2$ K). Bottom inset: dependence of $\Delta\rho_{xx}/\rho_{xx}$ on $1/B$ after subtraction of a background linear in B, i.e., $\Delta\rho_{xx}/\rho_{xx}-\alpha B$, where α is a constant. The asterisk indicates a spin splitting effect. Dashed lines are guides to the eye. Top inset: geometry of the magneto-transport experiment.

background linear in B. Maxima in $\Delta\rho_{xx}/\rho_{xx}$ correspond to resonant peaks in the oscillatory component of $\rho_{xx}(B)$; they are periodic in $1/B$ and quench very rapidly at $T>10$ K.

The different dependence on temperature of the negative MR and magneto-oscillations compared to the linear MR indicate that these effects have a different nature, i.e., they arise from quantum and classical phenomena, respectively. We first consider the oscillatory component of $\rho_{xx}(B)$. As shown in Fig. 3 for an $InAs_{1-x}N_x$ epilayer with $x=0.2\%$, the magneto-oscillations are observed for $B//z$ and for magnetic fields tilted at an angle θ relative to the z axis. The positions in $1/B$ of maxima/minima in ρ_{xx} scale as $1/B\cos\theta$, thus indicating that they are caused by the Shubnikov–de Haas effect in a two-dimensional electron gas (2DEG), which we attribute to the presence of a surface accumulation layer. Also, note the splitting of the maximum in ρ_{xx} at $1/B \sim 0.15$ T^{-1}, marked by an asterisk in the inset of Fig. 3. This splitting becomes more pronounced at larger θ. We attribute it to the spin-splitting of the $n=1$ Landau level (LL) of the 2DEG. In contrast to the orbital LL splitting, the spin splitting is determined by the magnitude of B, rather than by the component of B along z.[29] With increasing θ, the $n=1$ LL shifts toward higher values of B, and correspondingly the amplitude of the spin splitting increases.

Although 2DEG magneto-oscillations were reported before for $InAs_{1-x}N_x/In_yGa_{1-y}As$ quantum wells grown on InP,[30] to our knowledge they have not been reported previously for $InAs_{1-x}N_x$ epilayers on GaAs. On the other hand, it is well known that a 2DEG can form on the surface of narrow-gap semiconductors, such as InAs, due to the bending of the conduction band by charge on native surface defects with energy levels above the CB minimum.[20,21] For $x=0.2\%$, the SdH oscillations in ρ_{xx} occur at magnetic fields as low as $B_{2D}\sim 1$ T, providing us with an estimate of the 2DEG electron mobility $\mu_{2D}=B_{2D}^{-1}\sim 10^4$ $cm^2\,V^{-1}\,s^{-1}$ at $T=2$ K. The positions in $1/B\cos\theta$ of the ρ_{xx} maxima (or minima) plotted as a function of the integer n fall on a straight line. The period $B_f^{-1}=\Delta(1/B)=(0.15\pm 0.01)T^{-1}$, in the maxima or minima of ρ_{xx} gives an electron sheet density $n_{2D}=2e/h\Delta=3.2\times 10^{11}$ cm^{-2}. All our $InAs_{1-x}N_x$ layers showed similar, although less well resolved, low-temperature magneto-oscillations with a period $B_f^{-1}=\Delta(1/B)$ between 0.08 to 0.15 T^{-1} at $T=2$ K. This corresponds to electron sheet densities n_{2D} in the range from 6.0×10^{11} to 3.2×10^{11} cm^{-2}.

Given the presence of a conducting surface accumulation layer, we need to consider carefully the contribution of the 2D surface electrons and of the electrons in the bulk to the overall conductivity and magnetoconductivity of our Hall bars. Our data indicate that, at low temperatures, the contribution of the 2DEG to the measured conductivity is small. We estimate the resistance, R_{2D}, of the 2DEG to be $R_{2D}=(L/w)/(n_{2D}e\mu_{2D})$, where $L=1250$ μm and $w=250$ μm are the length and width of our Hall bars, respectively. For $x=0.2\%$, $B=0$ T and $T=2$ K, $R_{2D}\sim 10^4$ Ω, which is more than one order of magnitude higher than the measured resistance $R\sim 400$ Ω. Hence, the bulk electrons dominate the conductivity. Also, we note that, at all values of B and T, the amplitude of the magneto-oscillations is much smaller than the measured magnetoresistance; this indicates that the large linear MR observed in our samples originates mainly from the effect of B on the carriers in the bulk of the $InAs_{1-x}N_x$ epilayer.

A possible explanation of a positive transverse linear MR is that at high enough magnetic field, the electron distribution enters the so-called quantum limit, in which only the lowest-Landau level is occupied. This occurs when the cy-

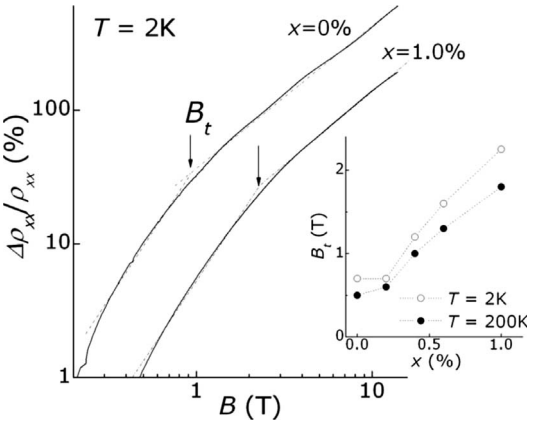

FIG. 4. B dependence of the MR for $x=0$ and $x=1\%$ ($T=2$ K). Dashed lines show the B^2 and linear B dependence of the MR. Inset: dependence on x of the magnetic field, B_t, for the crossover of the MR to a linear B dependence at $T=2$ and 200 K.

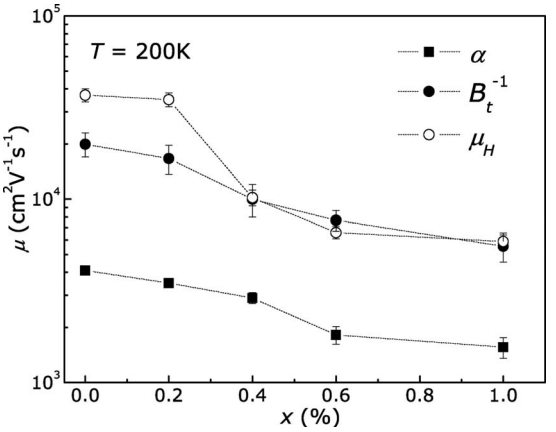

FIG. 5. Dependence on x of B_t^{-1}, α, and μ_H at $T=200$ K. Dashed lines are guides to the eye.

clotron energy, $\hbar\omega_c$, exceeds the Fermi energy, E_F, and $\hbar\omega_c$, $E_F \gg k_B T$.[31] However, this phenomenon cannot explain our linear MR, first because it is observed over a wide range of temperatures, $k_B T \gg \hbar\omega_c$, and, second, because it appears at low B. As shown in Fig. 1, in all samples the transition to a linear B dependence occurs at magnetic fields ($B \sim 1$ T) well below that corresponding to the quantum limit condition $\hbar\omega_c = E_F$, i.e., $B = \hbar(3\pi^2 n_e)^{2/3}/2e$. This corresponds to fields larger than 3 T for measured Hall densities $n_e > 3 \times 10^{16}$ cm^{-3} in our series of samples. We also note that the condition for single occupancy of the lowest Landau level requires that the temperature satisfies the condition $k_B T \ll \hbar\omega_c$. At $B=1$ T and for the electron cyclotron mass of InAs ($m_e^* = 0.0265 m_e$ at $T=4.2$ K),[32] this condition is satisfied for temperatures less than 50 K. However, as shown in Fig. 2, the positive linear MR is observed well above this temperature as well as below 50 K.

Linear MR effects of the type shown in Figs. 1 and 2 have been reported previously for other conductors, such as silver chalcogenides[33] and InSb,[34] and are presently of great interest for developing new magnetic sensors. In those materials, the linear transverse MR has been associated with distorted current paths and explained within a classical model in which the MR is controlled by disorder-induced macroscopic fluctuations, $\Delta\mu$, in the electron mobility.[35] In our $InAs_{1-x}N_x$ and InAs samples, a nonhomogenous concentration of threading dislocations formed at the highly mismatched $InAs_{1-x}N_x$/GaAs interface is likely to generate similar spatial fluctuations in the mobility. Highly disordered and dislocated interfaces were reported for InAs on GaAs[36] and can also exist in $InAs_{1-x}N_x$. In the classical MR model of Ref. 35, the crossover of the MR to a linear B dependence occurs at a threshold magnetic field $B_t = \bar{\mu}^{-1}$ for $\Delta\mu/\bar{\mu} < 1$ or at $B_t = \Delta\mu^{-1}$ for $\Delta\mu/\bar{\mu} > 1$. Here $\bar{\mu}$ corresponds to an average of the spatially varying mobility. Correspondingly, the magnitude of the MR is expected to scale with $\bar{\mu}$ for $\Delta\mu/\bar{\mu} < 1$ or with $\Delta\mu$ for $\Delta\mu/\bar{\mu} > 1$. We apply this model to our MR data and derive the value of B_t from the crossing of the B^2 and linear B dependences in the $\Delta\rho_{xx}/\rho_{xx}(B)$ curve, see Fig. 4. As shown in the inset of Fig. 4, the value of B_t increases with increasing x at low ($T=4.2$ K) and high temperatures ($T=200$ K). In contrast, the slope, α, of the $\Delta\rho_{xx}/\rho_{xx}(B)$ curve at high-B decreases with x, see Fig. 1.

We now compare the values of B_t^{-1} and α with the measured Hall mobilities, μ_H, derived from Hall measurements with B up to 0.4 T, corresponding to a range of B in which the Hall coefficient remains constant. As shown in Fig. 5, the values of μ_H, B_t^{-1} and α all exhibit a similar dependence on x. This supports the classical model of transverse linear MR in which the crossover to a linear B dependence occurs at $B_t = \bar{\mu}^{-1}$ and the slope, α, of the linear MR scales with $\bar{\mu}$ for $\Delta\mu/\bar{\mu} < 1$. The linear MR effect follows closely the T-dependence of μ_H. As shown in Fig. 6, at all temperatures the Hall mobility decreases with increasing N content, as is also observed for the magnitude of the linear MR. In particular, an increase of T above 10 K and up to ~150 K ($x=0\%$, 0.2%, and 0.4%) and 300 K ($x=0.6$ and 1%) leads to an increase of both μ_H and $\Delta\rho_{xx}/\rho_{xx}$. Only in samples with low x, does an increase of temperature above ~150 K cause

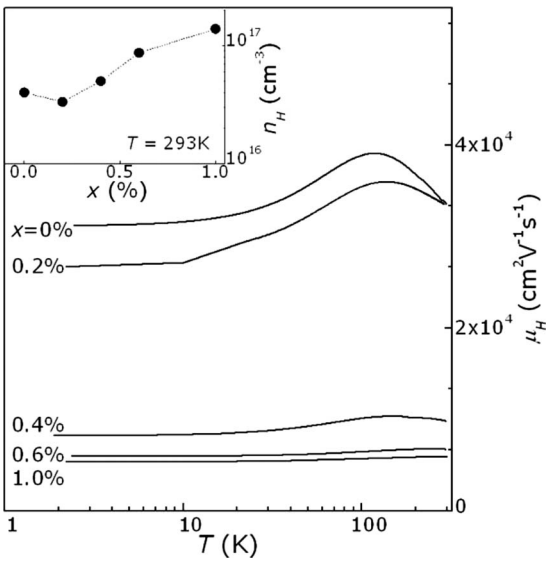

FIG. 6. Hall mobility, μ_H, versus T for all $InAs_{1-x}N_x$ samples. Inset: dependence on x of the electron Hall density, n_H ($T=293$ K). The dashed line is a guide to the eye.

a drop of μ_H and $\Delta\rho_{xx}/\rho_{xx}$. This effect, which we attribute to inelastic scattering by phonons, is not observed for $x > 0.4\%$, thus indicating that elastic scattering is dominant at these high x values, even at room temperature. The dominant contribution of impurity scattering at large x leads to a weaker T dependence of the linear MR in samples with $x > 0.4\%$ (inset of Fig. 2).

We attribute the decrease of electron mobility and magnitude of the linear MR with increasing x to scattering of the electrons by random alloy disorder[22,23] and by crystal defects. We note that the measured bulk electron densities in the nominally undoped $InAs_{1-x}N_x$ imply a fairly high density of native donor impurities. As shown in the inset of Fig. 6, the electron Hall density n_H increases from $\sim 4 \times 10^{16}$ cm^{-3} for $x=0\%$, 0.2%, and 0.4% to $\sim 1 \times 10^{17}$ m^{-3} for $x=0.6$ and 1% and $T=293$ K. Since our layers are not intentionally doped with donors, the measured increase of the electron density at $x > 0.4\%$ suggests that the N atoms act to increase the density of native donors, an effect also reported in previous studies.[16–18] This phenomenon may be related in part to the shift of native donor states into the conduction band as x increases and is supported by our photoluminescence studies revealing optical transitions with energies higher than the band gap of $InAs_{1-x}N_x$.[26] These states may arise from crystal defects caused by the nitrogen plasma and the low-growth temperature.[24,25] In the next section, we use cyclotron resonance experiments to investigate further the effect of the nitrogen and of composition disorder on the electronic properties.

IV. CYCLOTRON RESONANCE

We carried out the cyclotron resonance experiments by measuring the change in transmission of IR light from a quantum cascade laser as a function of the applied magnetic field. Figure 7 shows the magnetotransmission spectra at $T = 100$ K and laser wavelength $\lambda = 103$ μm for our $InAs_{1-x}N_x$ samples with $x=0$, 0.4, 0.6 and 1%. Each spectrum reveals a minimum, L1, at a resonance field $B_c \sim 3$ T that shifts to higher values of B with increasing x. For the layer with $x = 1\%$, we also observe an additional line, L2, at $B_c \sim 6$ T. Both resonances are more clearly resolved in the magnetotransmission spectrum measured with a shorter laser wavelength $\lambda = 75$ μm, see inset of Fig. 7.

We first consider samples with $x < 1\%$. From the temperature dependence of the magnetotransmission spectra, we infer that the L1 minimum arises from free-electron cyclotron resonance absorption, rather than from impurities-related CR. The measured change in the B position and linewidth of the L1 line reveals an increase in the electron cyclotron mass, m_e^*, and a corresponding decrease of the scattering time, τ, with increasing x. To deduce the values of m_e^* and τ, we fit the L1 minimum by a Lorentzian curve after subtracting from the magnetotransmission spectrum a background that is linear in B. This background accounts for the free carrier absorption and its B dependence at high B.[37] Our analysis of the CR lineshape gives a sheet density of resonating carriers $n_s > 4 \times 10^{12}$ cm^{-2}. The density values are close to the measured Hall densities ($n_H > 3 \times 10^{12}$ cm^{-2}),

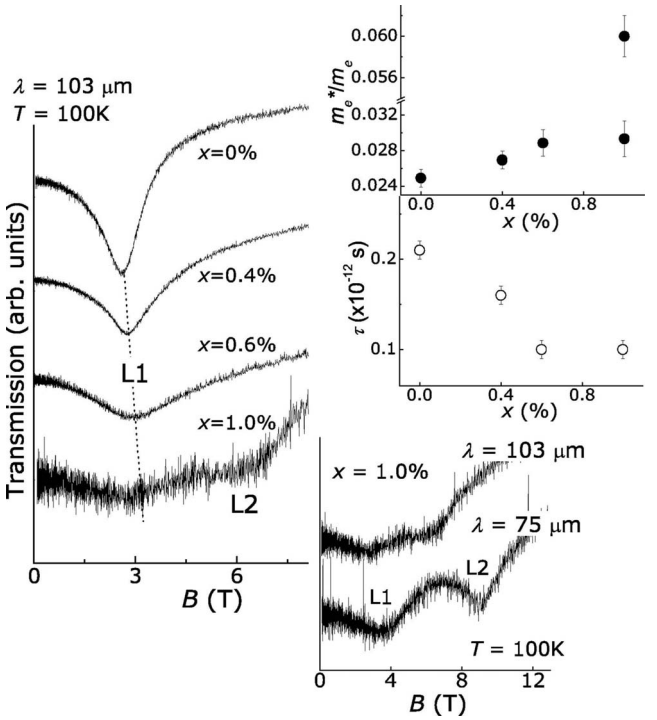

FIG. 7. Cyclotron resonance spectra in magnetotransmission for the $InAs_{1-x}N_x$ samples with $x=0\%$, 0.4%, 0.6%, and 1.0% ($T = 100$ K and $\lambda = 103$ μm). Bottom inset: Magneto-transmission spectra at $\lambda = 103$ and 75 μm for the $InAs_{1-x}N_x$ sample with $x = 1.0\%$ ($T = 100$ K). Top inset: x dependence of the electron cyclotron mass and scattering time at $T = 100$ K and $\lambda = 103$ μm.

but are much larger than the sheet densities in the accumulation layer ($n_{2DEG} < 6 \times 10^{11}$ cm^{-2}), thus indicating that the L1 minimum is due to the bulk $InAs_{1-x}N_x$ epilayer. This is further supported by CR experiments in which the magnetic field is tilted at angle θ relative to the growth axis z. These experiments show that tilting θ by up to 30° does not change the B-position or shape of the L1 line, from which we deduce that the motion of the resonating carriers is not confined to two dimensions.

For pure InAs, we find that $m_e^* = (0.025 \pm 0.001) m_e$ at $T = 100$ K and $\lambda = 103$ μm, where m_e is the electron mass in vacuum. This value of m_e^* is in agreement with previous studies of the electron mass in pure InAs[32] and with that measured for InAs on GaAs [$m_e^* = (0.0236 \pm 0.0003) m_e$].[21] As shown in the inset of Fig. 7, the value of m_e^* increases with x up to $m_e^* = (0.029 \pm 0.002) m_e$ at $x=0.6\%$. Our measured increase of m_e^* ($\sim 16\%$) is larger than that ($< 10\%$) predicted by a two-level band anticrossing model[1] with parameters for $InAs_{1-x}N_x$ from Ref. 5. An even stronger enhancement of the electron effective mass has been reported for $InAs_{1-x}N_x$ epilayers on InP using reflectivity measurements[38] and for $InAs_{1-x}N_x$/InGaAs quantum wells on InP,[39] in which an effective mass $m_e^* > 0.04 m_e$ was found even at x as low as 0.2%. The apparent discrepancy between our CR data and previous estimates[38,39] can be explained by noting that the latter were made on epilayers with high-electron densities, i.e., $n_e > 10^{18}$ cm^{-3}, or on thin quantum wells. In the case of heavily doped epilayers,[38] the Fermi

energy lies well above (>100 meV) the conduction band edge, where nonparabolicity effects and mass enhancements can be strong. In the case of quantum wells, the electron mass can be enhanced by quantization effects.[39] The enhancement of the electron mass in $InAs_{1-x}N_x$ has been attributed to the interaction of the N levels with the conduction band states of InAs, thus, leading to states with admixed character,[38,39] as already observed for other dilute nitride alloy systems.[5,40,41] We also note that electron localization phenomena due to the N incorporation can affect the electron mass as discussed below for the $InAs_{1-x}N_x$ sample with $x=1\%$.

For the $InAs_{1-x}N_x$ epilayer with $x=1\%$, we observe two CR minima, L1 and L2. The mass corresponding to L1 is $m_e^*=(0.029\pm0.002)m_e$ and tends to follow the monotonic increase of m_e^* with increasing x shown in Fig. 7 for samples with lower x. In contrast, L2 corresponds to a much larger cyclotron mass $m_e^*=(0.060\pm0.002)m_e$. Since in this sample the L1 line disappears as B is tilted relative to the growth axis, z, whereas L2 is observed at different angles and at the same resonant field, we infer that only the L2 resonance arises from the $InAs_{1-x}N_x$ bulk epilayer. The large N-induced mass enhancement observed at $x=1\%$ suggests an unusual distortion of the upper $(n=1,2)$ Landau levels due to localized energy levels resonant with the conduction band states. Our Hall effect measurements show a relatively large residual electron concentration in this sample, i.e., $n_H=2\times10^{17}$ cm^{-3}, due to native donor states; consistent with this, PL experiments have indicated the existence of localized energy levels that are resonant with the conduction band states.[26] Since N-N pairs in InAs are expected to be high in energy relative to the conduction band minimum (>1 eV), we propose that other defects could be responsible for these localized states, such as N clusters with lower energies and/or native defects that shift into the conduction band due to the N incorporation. This phenomenon merits further investigation, for example by studying the resonant magnetotransmission over a wider range of terahertz frequencies.

As shown in Fig. 7, in $InAs_{1-x}N_x$ the linewidth of the CR lines broadens with increasing x, but CR lines can be observed even at $x=1\%$. For $x=0$ and $T=100$ K, the analysis of the CR lineshape gives $\tau\sim0.2$ ps corresponding to an effective mobility $\mu_{CR}\sim1.6\times10^4$ cm^2 V^{-1} s^{-1}. The scattering time decreases with x down to a value of $\tau\sim0.1$ ps at $x=1\%$ ($\mu_{CR}\sim6\times10^3$ cm^2 V^{-1} s^{-1}), see inset of Fig. 7. The decrease in τ and μ_{CR} at high x is in agreement with that shown in Fig. 5 for B_t^{-1}, α and the Hall mobility, μ_H. The measured dependence of the electron mobility on x is much weaker than that found in our $GaAs_{1-x}N_x$ epilayers in which the CR lines and electron mobility quench very rapidly at $x>0\%$.[19]

To date there have been only a few reports of CR in III-N-V compounds.[40,42] For $GaAs_{1-x}N_x$, clear CR absorptions were only observed up to $x\sim0.1\%$,[40] while CR absorptions were measured in the narrow gap $InSb_{1-x}N_x$ alloy at $x=1\%$.[42] These previous studies and our data in $InAs_{1-x}N_x$ underline qualitative differences between wide and narrow III-N-V alloys. In particular, in $GaAs_{1-x}N_x$, the localized electron states of N-atom and N-N pairs are close to the conduction band edge (~0.1 eV),[2,3,5] thus acting as strong resonant scattering centers and suppressing the electron mobility at values of x as small as 0.1%.[19,40,22,23] In contrast, in $InAs_{1-x}N_x$, as well as in other narrow gap alloys such as $InSb_{1-x}N_x$, these states are expected to be at higher energies (~1 eV) in the conduction band.[5] Correspondingly, the perturbation of the band states by the nitrogen and the strength of resonant scattering are weaker.

The Γ-like conduction band character and delocalization of the electronic states in these $InAs_{1-x}N_x$ epilayers is further supported by the negative MR effect shown in the inset of Fig. 1. The negative MR is a weak localization (WL) effect and is commonly observed in disordered conductors at low temperatures.[43] The magnetic field breaks the time-reversal symmetry of the electron waves, thus, destroying the coherent backscattering of electrons due to quantum interference, and leading to a quenching of weak localization and a decrease in the resistance. This process is determined by a characteristic coherence length, $l_\varphi=(D\tau_\varphi)^{1/2}$. Here, $D=v_F^2\tau/3$ is the diffusion coefficient, τ_φ is the coherence time, τ is the elastic scattering time and v_F is the electron velocity at the Fermi energy.[43] For weak localization of extended states, the negative MR deviates from the characteristic B^2 dependence when the magnetic length, $l_c=\sqrt{\hbar/eB}$, becomes comparable to $2l_\varphi$. Using this criterion and the measured negative MR at low $B(<0.1$ T), we estimate an electron coherent length $l_\varphi\sim80$ nm at $x=0$ and $T=2$ K. Our measurements on the layers indicates that the value of l_φ tends to decrease with increasing N content, but remains relatively high ($L_\varphi\sim60$ nm) even for $x=1\%$.

Finally, we note that an antiweak localization (AWL) effect has been reported previously in InAs.[44,45] This arises from spin-orbit interaction and spin-dephasing and appears as a cusp-like minimum in the $\rho_{xx}(B)$ plot for very weak fields (~mT) around $B=0$. We were unable to observe this signature of AWL in the magnetoresistance plots of any of our samples within the resolution of 10 mT in our measurement system.

V. CONCLUSIONS

In conclusion, transverse magnetoresistance, ρ_{xx}, Hall effect and transmission cyclotron resonance measurements of $InAs_{1-x}N_x$ epilayers grown on GaAs have provided detailed information about the effects of the N incorporation on the electronic properties of the small gap semiconductor InAs. All samples showed a weak negative transverse magnetoresistance at $B<0.1$ T followed at higher fields ($B>1$ T) by a positive linear MR and by a weak oscillatory modulation of ρ_{xx}. We attribute the magneto-oscillations in ρ_{xx} to the Shubnikov–de Haas effect in the surface electron accumulation layer. The linear MR is instead a classical effect due to inhomogeneities in the bulk $InAs_{1-x}N_x$ epilayer and its magnitude and temperature dependence are controlled by the N content. Our analysis of the MR and of the Hall measurements showed that the electrical conductivity in $InAs_{1-x}N_x$ retains the characteristic features of transport through extended Γ-like conduction band states with electron coherence lengths and electron mobilities that remain high even at $x=1\%$. Correspondingly, the cyclotron resonance studies re-

vealed sharp cyclotron resonance lines and a systematic increase of the electron cyclotron mass with increasing x. This behavior differs from that observed in other dilute nitride alloys, such as $GaAs_{1-x}N_x$, where carrier localization onto N-related states act to fragment the conduction band and degrade the electrical conductivity even at $x \sim 0.1\%$. Further studies are now needed to probe the effect of higher N-concentrations ($>1\%$) and to explore in more detail the strong mass enhancement indicated by our CR experiments in the $InAs_{1-x}N_x$ alloy with $x=1\%$. The high quality of $InAs_{1-x}N_x$ epilayers on GaAs and the tunability of fundamental band parameters by the N-incorporation should stimulate further experimental and theoretical work. Models of the electronic properties of $InAs_{1-x}N_x$ are required to assess the effect of the nitrogen on the conduction band structure, particularly at large k vectors. The low disorder revealed in our measurements also suggests realistic prospects for the implementation of $InAs_{1-x}N_x$ in GaAs-based heterostructures.

ACKNOWLEDGMENTS

This work has been supported by EuroMagNET under EU Contract No. RII3-CT-2004-506239, the Engineering and Physical Sciences Research Council (UK), the Royal Society (UK), and the Coordenação de Aperfeiçoamento de Pessoal de Nível Superior, CAPES (Brazil). We acknowledge useful discussions with G. Allison and J. Wosnitza. We are grateful to G. Fasching for providing us with the quantum cascade lasers.

*Corresponding author. amalia.patane@nottingham.ac.uk

[1] W. Shan, W. Walukiewicz, J. W. Ager, E. E. Haller, J. F. Geisz, D. J. Friedman, J. M. Olson, and S. R. Kurtz, Phys. Rev. Lett. **82**, 1221 (1999).
[2] P. R. C. Kent and A. Zunger, Phys. Rev. B **64**, 115208 (2001).
[3] A. Lindsay and E. P. O'Reilly, Phys. Rev. Lett. **93**, 196402 (2004).
[4] J. Li, P. Carrier, S. H. Wei, S. S. Li, and J. B. Xia, Phys. Rev. Lett. **96**, 035505 (2006).
[5] E. P. O'Reilly, A. Lindsay, P. J. Klar, A. Polimeni, and M. Capizzi, Semicond. Sci. Technol. **24**, 033001 (2009).
[6] K. M. Yu, W. Walukiewicz, J. Wu, D. E. Mars, D. R. Chamberlin, M. A. Scarpulla, O. D. Dubon, and J. F. Geisz, Nature Mater. **1**, 185 (2002).
[7] A. R. Adams, Electron. Lett. **40**, 1086 (2004).
[8] A. Ignatov, A. Patanè, O. Makarovsky, and L. Eaves, Appl. Phys. Lett. **88**, 032107 (2006).
[9] M. Felici, A. Polimeni, G. Salviati, L. Lazzarini, N. Armani, F. Masia, M. Capizzi, F. Martelli, M. Lazzarino, G. Bais, M. Piccin, S. Rubini, and A. Franciosi, Adv. Mater. **18**, 1993 (2006).
[10] H. Naoi, Y. Naoi, and S. Sakai, Solid-State Electron. **41**, 319 (1997).
[11] T. D. Veal, L. F. J. Piper, P. H. Jefferson, I. Mahboob, C. F. McConville, M. Merrick, T. J. C. Hosea, B. N. Murdin, and M. Hopkinson, Appl. Phys. Lett. **87**, 182114 (2005).
[12] Q. Zhuang, A. M. R. Godenir, A. Krier, K. T. Lai, and S. K. Haywood, J. Appl. Phys. **103**, 063520 (2008).
[13] S. Dhar, T. D. Das, M. de la Mare, and A. Krier, Appl. Phys. Lett. **93**, 071905 (2008).
[14] H. Benaissa, A. Zaoui, and M. Ferhat, J. Appl. Phys. **102**, 113712 (2007).
[15] M. Merrick, S. A. Cripps, B. N. Murdin, T. J. C. Hosea, T. D. Veal, C. F. McConville, and M. Hopkinson, Phys. Rev. B **76**, 075209 (2007).
[16] M. Kuroda, R. Katayama, S. Nishio, K. Onabe, and Y. Shiraki, Phys. Status Solidi C **0**, 2765 (2003).
[17] S. Kuboya, F. Nakajima, R. Katayama, and K. Onabe, Phys. Status Solidi B **243**, 1411 (2006).
[18] D.-K. Shih, H.-H. Lin, L.-W. Sung, T.-Y. Chu, and T.-R. Yang, Jpn. J. Appl. Phys. **42**, 375 (2003).
[19] A. Patanè, G. Allison, L. Eaves, N. V. Kozlova, Q. D. Zhuang, A. Krier, M. Hopkinson, and G. Hill, Appl. Phys. Lett. **93**, 252109 (2008); D. Fowler, O. Makarovsky, A. Patanè, L. Eaves, L. Geelhaar, and H. Riechert, Phys. Rev. B **69**, 153305 (2004).
[20] D. C. Tsui, Solid State Commun. **9**, 1789 (1971).
[21] P. D. Wang, S. N. Holmes, T. Le, R. A. Stradling, I. T. Ferguson, and A. G. Oliveira, Semicond. Sci. Technol. **7**, 767 (1992).
[22] S. Fahy, A. Lindsay, H. Ouerdane, and E. P. O'Reilly, Phys. Rev. B **74**, 035203 (2006).
[23] M. P. Vaughan and B. K. Ridley, Phys. Rev. B **75**, 195205 (2007).
[24] M. M. Oye, T. J. Mattord, G. A. Hallock, S. R. Bank, M. A. Wistey, J. M. Reifsnider, A. J. Ptak, H. B. Yuen, J. S. Harris, and A. L. Holmes, Appl. Phys. Lett. **91**, 191903 (2007).
[25] S. R. Bank, H. Bae, L. L. Goddard, H. B. Yuen, M. A. Wistey, R. Kudrawiec, and J. S. Harris, IEEE J. Quantum Electron. **43**, 773 (2007).
[26] M. de la Mare, Q. Zhuang, A. Krier, A. Patanè, and S. Dhar, Appl. Phys. Lett. **95**, 031110 (2009).
[27] R. Köhler, A. Tredicucci, F. Beltram, H. E. Beere, E. H. Linfield, A. G. Davies, D. A. Ritchie, R. C. Iotti, and F. Rossi, Nature (London) **417**, 156 (2002).
[28] S. Barbieri, J. Alton, H. E. Beere, J. Fowler, E. H. Linfield, and D. A. Ritchie, Appl. Phys. Lett. **85**, 1674 (2004).
[29] D. R. Leadley, R. J. Nicholas, J. J. Harris, and C. T. Foxon, Phys. Rev. B **58**, 13036 (1998).
[30] D. R. Hang, C. F. Huang, W. K. Hung, Y. H. Chang, J. C. Chen, H. C. Yang, Y. F. Chen, D. K. Shih, T. Y. Chu, and H. H. Lin, Semicond. Sci. Technol. **17**, 999 (2002).
[31] A. A. Abrikosov, Sov. Phys. JETP **29**, 746 (1959); J. Phys. A **36**, 9119 (2003).
[32] O. Madelung, *Semiconductors: Data Handbook* (Springer, London, 2003).
[33] R. Xu, A. Husmann, T. F. Rosenbaum, M.-L. Saboungi, J. E. Enderby, and P. B. Littlewood, Nature (London) **390**, 57 (1997).
[34] J. Hu and T. F. Rosenbaum, Nature Mater. **7**, 697 (2008).
[35] M. M. Parish and P. B. Littlewood, Nature (London) **426**, 162 (2003); Phys. Rev. B **72**, 094417 (2005).
[36] T. Kawai, H. Yonezu, D. Saito, M. Yokozeki, and K. Pak, Jpn. J. Appl. Phys. **33**, L1740 (1994).

[37] M. P. Semtsiv, S. Dressler, W. T. Masselink, V. V. Rylkov, J. Galibert, M. Goiran, and J. Leotin, Phys. Rev. B **74**, 041303(R) (2006).
[38] W. K. Hung, K. S. Cho, M. Y. Chern, Y. F. Chen, D. K. Shih, H. H. Lin, C. C. Lu, and T. R. Yang, Appl. Phys. Lett. **80**, 796 (2002).
[39] D. R. Hang, D. K. Shih, C. F. Huang, W. K. Hung, Y. H. Chang, Y. F. Chen, and H. H. Lin, Physica E **22**, 308 (2004).
[40] R. Mouillet, L.-A. de Vaulchier, E. Deleporte, Y. Guldner, L. Travers, and J. C. Harmand, Solid State Commun. **126**, 333 (2003).
[41] G. Allison, S. Spasov, A. Patanè, L. Eaves, N. Koslova, J. Freudemberger, M. Hopkinson, and G. Hill, Phys. Rev. B **77**, 125210 (2008).
[42] B. N. Murdin, A. R. Adams, P. Murzyn, C. R. Pidgeon, I. V. Bradley, J. P. R. Wells, Y. H. Matsuda, N. Miura, T. Burke, and A. D. Johnson, Appl. Phys. Lett. **81**, 256 (2002).
[43] P. A. Lee and T. V. Ramakrishnan, Rev. Mod. Phys. **57**, 287 (1985).
[44] G. L. Chen, J. Han, T. T. Huang, S. Datta, and D. B. Janes, Phys. Rev. B **47**, 4084 (1993).
[45] Ch. Schierholz, R. Kursten, G. Meier, T. Matsuyama, and U. Merkt, Phys. Status Solidi B **233**, 436 (2002).